

Brain anomalies in children exposed prenatally to a common organophosphate pesticide

Virginia A. Rauh^{a,b,1}, Frederica P. Perera^{b,c}, Megan K. Horton^{b,d}, Robin M. Whyatt^{b,c}, Ravi Bansal^e, Xuejun Hao^e, Jun Liu^e, Dana Boyd Barr^f, Theodore A. Slotkin^g, and Bradley S. Peterson^{e,h}

^aHeilbrunn Center for Population and Family Health, ^bColumbia Center for Children's Environmental Health, and Departments of ^cEnvironmental Health Sciences and ^dEpidemiology, Mailman School of Public Health, Columbia University, New York, NY 10032; ^eDivision of Child and Adolescent Psychiatry, Columbia University College of Physicians and Surgeons, New York, NY 10032; ^fRollins School of Public Health, Emory University, Atlanta, GA 30322; ^gDepartment of Pharmacology and Cancer Biology, Duke University Medical Center, Durham, NC 27710; and ^hDepartment of Child and Adolescent Psychiatry, New York State Psychiatric Institute, New York, NY 10032

Edited by James L. McGaugh, University of California, Irvine, CA, and approved March 30, 2012 (received for review February 27, 2012)

Prenatal exposure to chlorpyrifos (CPF), an organophosphate insecticide, is associated with neurobehavioral deficits in humans and animal models. We investigated associations between CPF exposure and brain morphology using magnetic resonance imaging in 40 children, 5.9–11.2 y, selected from a nonclinical, representative community-based cohort. Twenty high-exposure children (upper tertile of CPF concentrations in umbilical cord blood) were compared with 20 low-exposure children on cortical surface features; all participants had minimal prenatal exposure to environmental tobacco smoke and polycyclic aromatic hydrocarbons. High CPF exposure was associated with enlargement of superior temporal, posterior middle temporal, and inferior postcentral gyri bilaterally, and enlarged superior frontal gyrus, gyrus rectus, cuneus, and precuneus along the mesial wall of the right hemisphere. Group differences were derived from exposure effects on underlying white matter. A significant exposure × IQ interaction was derived from CPF disruption of normal IQ associations with surface measures in low-exposure children. In preliminary analyses, high-exposure children did not show expected sex differences in the right inferior parietal lobule and superior marginal gyrus, and displayed reversal of sex differences in the right mesial superior frontal gyrus, consistent with disruption by CPF of normal behavioral sexual dimorphisms reported in animal models. High-exposure children also showed frontal and parietal cortical thinning, and an inverse dose–response relationship between CPF and cortical thickness. This study reports significant associations of prenatal exposure to a widely used environmental neurotoxicant, at standard use levels, with structural changes in the developing human brain.

brain structure | neurotoxicity

Chlorpyrifos (CPF) is a widely used, broad-spectrum organophosphate insecticide first registered in 1965 for agricultural uses and pest control. Before regulatory action by the Environmental Protection Agency that phased out residential use in 2001 (1), CPF applications were particularly heavy in urban areas, where exposed populations included pregnant women (2, 3). CPF remains heavily used in agriculture, with continuing exposures of workers and residents of agricultural communities, as well as the general population through consumption of CPF-treated agricultural products. The major concern for human health is the propensity of organophosphate insecticides to elicit neurodevelopmental toxicity. Animal studies show that developmental exposures to CPF have adverse effects on brain development and produce neurobehavioral abnormalities at exposures well below the threshold for systemic toxicity caused by cholinesterase inhibition, the biochemical measure most commonly used to assess exposure and safety (4). A major component of the neurodevelopmental toxicity of CPF is likely to be unrelated to its ability to inhibit cholinesterase, instead involving disruption of the cellular machinery controlling

neuronal replication and differentiation, apoptosis, axon formation, synaptogenesis, and neural circuit formation (4, 5).

The effects of low-level organophosphate exposures on brain development in animal models triggered a series of studies in children to examine whether purportedly “safe” exposure levels had consequences similar to those in animals. Organophosphate insecticides in humans are detectable in amniotic fluid (6) and readily cross the placenta (7). Prenatal exposures to CPF and other organophosphate pesticides have been linked to smaller head size (8), lower birth weight (9), deviant neonatal reflexes (10, 11), attention problems (12, 13), and neurodevelopmental anomalies resembling pervasive development disorder (13, 14) in preschool-aged children. Three recent studies undertaken by different research groups all concluded that prenatal organophosphate exposure is associated with a significant reduction in childhood IQ (15–17). These studies, using different biomarkers of exposure (urinary metabolites, umbilical cord blood), show that prenatal organophosphate exposure produces a consistent pattern of early cognitive and behavioral deficits across both agricultural and urban populations.

Despite this converging evidence for the neurodevelopmental toxicity of organophosphate insecticides, their specific effects on brain structure that disrupt behavior and cognition in humans are unknown. The few animal studies that have examined morphological consequences of early life organophosphate exposure indicate subtle changes in cortical thickness and neuronal and glial cell proportions in the septal nucleus, striatum, somatosensory cortex, and hippocampus—brain regions that subserve mood, behavior, and cognition (18, 19). These studies have shown CPF effects on glial cell numbers, changes in number and types of neurons in all four regions, as well as delayed alterations in hippocampal cell number accompanied by perikaryal swelling and excessive astrocytic processes, likely representing early stages of astrogliosis, the glial scarring that occurs in response to cellular injury—all at a dose too low for signs of systemic toxicity (19). Consistent with these glial-based effects of early postnatal exposure, prenatal exposure to CPF has been shown to increase the levels of glial cell markers in rodents (20). Notably, early life CPF exposure interferes with normal sexual differentiation of the brain, reducing or reversing the normal sex differences in cognitive and emotion-related behaviors (21, 22) and correlating with sex-specific effects on the neurotransmitter systems that support those behaviors.

Author contributions: V.A.R., F.P.P., R.M.W., T.A.S., and B.S.P. designed research; M.K.H., R.B., X.H., and J.L. performed research; D.B.B. contributed new reagents/analytic tools; R.B., X.H., and J.L. analyzed data; and V.A.R., R.B., T.A.S., and B.S.P. wrote the paper.

Conflict of interest statement: T.A.S. has provided expert testimony on the health effects of chlorpyrifos on behalf of government entities, corporations, and/or individuals.

This article is a PNAS Direct Submission.

¹To whom correspondence should be addressed. E-mail: var1@columbia.edu.

This article contains supporting information online at www.pnas.org/lookup/suppl/doi:10.1073/pnas.1203396109/-DCSupplemental.

In the current study, we compared morphological measures of the cerebral surface, as well as measures of the thickness of the cortical mantle, across two groups of children exposed prenatally to high or low levels of CPF. We assessed whether those regional abnormalities related to CPF exposure were associated with reductions in measures of intellectual functioning. We hypothesized that children exposed prenatally to high levels of CPF compared with those with low levels of exposure would have altered morphological characteristics in brain regions (frontal, parietal, and lateral temporal) that subservise higher-cognitive functions. We also assessed in preliminary analyses whether prenatal CPF exposure disrupted normal sex differences in brain structure in our sample of school-aged children.

Results

Sample Description. The sample was selected from a larger cohort of 369 children with complete prenatal CPF, polycyclic aromatic hydrocarbons (PAH), and environmental tobacco smoke (ETS) exposure data, and 7-y cognitive testing (WISC-IV). Of these children, 70 had CPF exposure levels in the upper tertile of the distribution (≥ 4.39 pg/g), 28 of whom also met the criteria of (i) no/very low prenatal ETS exposure, classified by maternal report and validated by cotinine levels < 15 ng/mL in umbilical cord blood (23); and (ii) low prenatal PAH exposure levels, measured by third-trimester personal monitoring, and defined as below the median (2.26 ng/m³). Of these 28 eligible high-exposure children, 20 completed the MRI with usable imaging data. For the low-exposure group, 99 had CPF below the upper tertile, PAH below the median, and no/very low ETS exposure. Of these, 38 were randomly selected and 20 completed the MRI with usable imaging data. Written informed consent was obtained from all parents and signed assent from all children. The Institutional Review Boards for the New York State Psychiatric Institute and Columbia University approved the study.

Table 1 compares high- and low-exposure groups, and the full sample with the larger cohort (all children with exposure data and

7-y testing) on selected characteristics. There were no significant differences between the study sample ($n = 40$) and the larger cohort ($n = 329$, excluding the study sample), or any significant differences between high- and low-exposure groups on any characteristic. CPF concentration was not significantly associated with lead in the study sample (Spearman's $\rho = 0.15$, $P = 0.46$) or the larger cohort (Spearman's $\rho = 0.07$; $P = 0.30$). The sample was largely full-term because of third-trimester air monitoring.

Effects on Morphology of the Cerebral Surface. *Main effects of exposure.* Overall brain size did not differ significantly across exposure groups, either unadjusted (high vs. low exposure $1,257.2 \pm 103.5$ vs. $1,247.9 \pm 77.6$ cm³, $t = 0.64$, $df = 37$, $P = 0.52$) or adjusted for age, sex, and height (high vs. low exposure $1,265.1 \pm 17.7$ vs. $1,242.1 \pm 16.8$, $F = 0.84$, $df = 1, 35$, $P = 0.37$). Nevertheless, the high-CPF group had significant enlargement bilaterally of the superior temporal, posterior middle temporal, and inferior postcentral gyri bilaterally; the supramarginal gyrus and inferior parietal lobule of the right hemisphere; and superior frontal gyrus, gyrus rectus, cuneus, and precuneus along the mesial wall of the right hemisphere, with or without correction for overall brain size (Fig. 1 and Figs. S1 and S2). Additional analyses of white matter surface demonstrated that this enlargement at the cerebral surface derived primarily from enlarged underlying white matter (Fig. S3). In addition, we detected inward deformations in the dorsal and mesial surfaces of the left superior frontal gyrus (Fig. 1). Within the high-CPF group, we found a significant positive dose-response relationship between exposure level and enlargement of the mesial surface of the superior frontal gyrus bilaterally.

IQ \times exposure interaction. We saw a significant IQ \times exposure interaction on surface measures in the superior temporal, inferior frontal, inferior precentral, and inferior postcentral gyri bilaterally, and the precuneus of the left hemisphere, such that IQ correlated positively with surface measures in the low- but

Table 1. Sociodemographic characteristics of the study sample by prenatal CPF exposure group, compared with the larger cohort from which the sample was selected

Characteristic*	High exposure	Low exposure	P^\dagger	Full sample	Larger cohort	P^\ddagger
	$n = 20$	$n = 20$		$n = 40$	$n = 329$	
	N (%)	N (%)		N (%)	N (%)	
	Mean \pm SD	Mean \pm SD		Mean \pm SD	Mean \pm SD	
Income						
<\$20,000	11 (55.0)	12 (60.0)	N.S.	23 (57.5)	170 (51.7)	N.S.
\geq \$20,000	9 (45.0)	8 (40.0)		17 (42.5)	159 (48.3)	
Maternal education, y [§]	12.9 \pm 2.5	13.4 \pm 2.9	N.S.	12.4 \pm 1.9	12.3 \pm 2.6	N.S.
Maternal IQ [¶]	87.5 \pm 12.6	89.8 \pm 10.0	N.S.	85.2 \pm 14.7	85.0 \pm 12.9	N.S.
Maternal race/ethnicity						
Dominican	11 (27.5)	14 (35.0)	N.S.	25 (62.5)	202 (61.4)	N.S.
African American	9 (22.5)	6 (15.0)		15 (37.5)	127 (38.6)	
Child sex						
Male	6 (30.0)	9 (45.0)	N.S.	15 (37.5)	155 (47.1)	N.S.
Female	14 (70.0)	11 (55.0)		25 (62.5)	174 (52.9)	
Gestational age, wk	39.3 \pm 1.4	39.3 \pm 2.5	N.S.	39.3 \pm 2.0	39.3 \pm 1.4	N.S.
Birth weight, g	3,199.5 \pm 625.0	3,362.9 \pm 509.6	N.S.	3,281.2 \pm 568.9	3,400 \pm 479.9	N.S.
Child age at MRI, y	8.5 \pm 1.2	7.8 \pm 0.9	N.S.	—	—	
Prenatal lead, μ g/dL	1.4 \pm 1.2	0.8 \pm 0.5	N.S.	1.1 \pm 0.9	1.2 \pm 0.9	N.S.

N.S., not significant.

*All maternal and family demographic characteristics assessed at child age 7 y.

[†]Comparison of high CPF exposed (≥ 4.39 pg/g) with low CPF exposed (< 4.39 pg/g); $P < 0.05$.

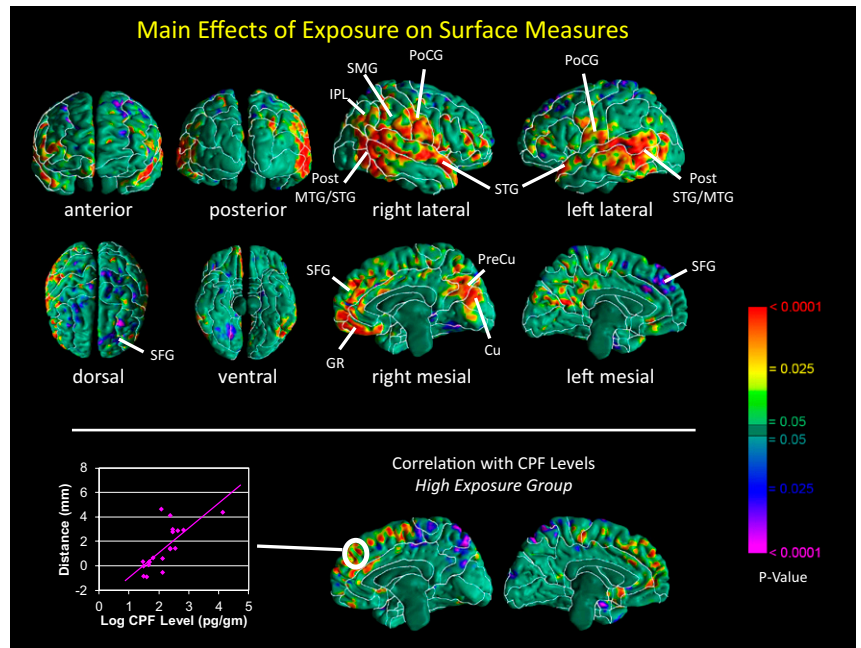
[‡]Comparison of study sample with cohort of all eligible children having prenatal exposure data for CPF, PAH, ETS, and 7-y cognitive assessments, minus study sample; $P < 0.05$.

[§]Years of education completed at child age 7.

[¶]Based on Brown et al. (53).

^{||}Umbilical cord-blood lead concentrations were available for a subset ($n = 28$) of study children (13 higher exposure; 15 lower exposure) and a subset of the larger cohort ($n = 202$).

Fig. 1. (Upper) Maps of exposure group differences in morphological measures of the cerebral surface. At each point on the cerebral surface of the template brain, we compared (i) average distance of the surface of each brain in the high-CPF group from the corresponding point on the surface of the template, with (ii) average distance of the surface of each brain in the low-CPF group from the same point on the surface of the template, adjusted for age and sex. Warm colors (yellow, orange, and red) indicate significantly larger distances (local enlargements, outward deformations) in high- vs. low-CPF group; cool colors (blue and purple) indicate reduced distances (indentations, inward deformations) in high- vs. low-CPF group. The color bar indicates *P* values, corrected for multiple comparisons using a false discovery rate $P < 0.05$. High-CPF group brains were significantly enlarged bilaterally in the superior temporal, posterior middle temporal, and inferior postcentral gyri, and superior frontal gyrus, gyrus rectus, cuneus, and precuneus in the mesial views of the right hemisphere. CU, cuneus; GR, gyrus rectus; MTG, middle temporal gyrus; PoCG, postcentral gyrus; PreCU, precuneus; SFG, superior frontal gyrus; STG, superior temporal gyrus. (Lower) Correlations of local surface measures with prenatal CPF exposure levels in the high-exposure group. Surface distances (in mm from the corresponding point on the surface of the template brain), adjusted for age and sex, are plotted on the y axis. Log-transformed CPF cord-blood levels (pg/g) are plotted on the x axis. Warm colors (red and yellow) indicate positive correlations, and cool colors (blue and purple) indicate inverse correlations between surface measures and CPF exposure. The scatterplot of individuals shows enlarged surfaces along the superior frontal gyrus with increasing exposure to CPF.



not the high-CPF group (Fig. 2). We also found a significant interaction in the right fusiform gyrus, where IQ correlated inversely with surface measures in the low-CPF group but positively in the high group (Fig. 2).

Sex \times exposure interaction. We found significant sex \times exposure interactions within the right inferior parietal lobule, right superior marginal gyrus, and right mesial superior frontal gyrus (Fig. 3), reflecting disruption of normal, female-larger-than-male sex

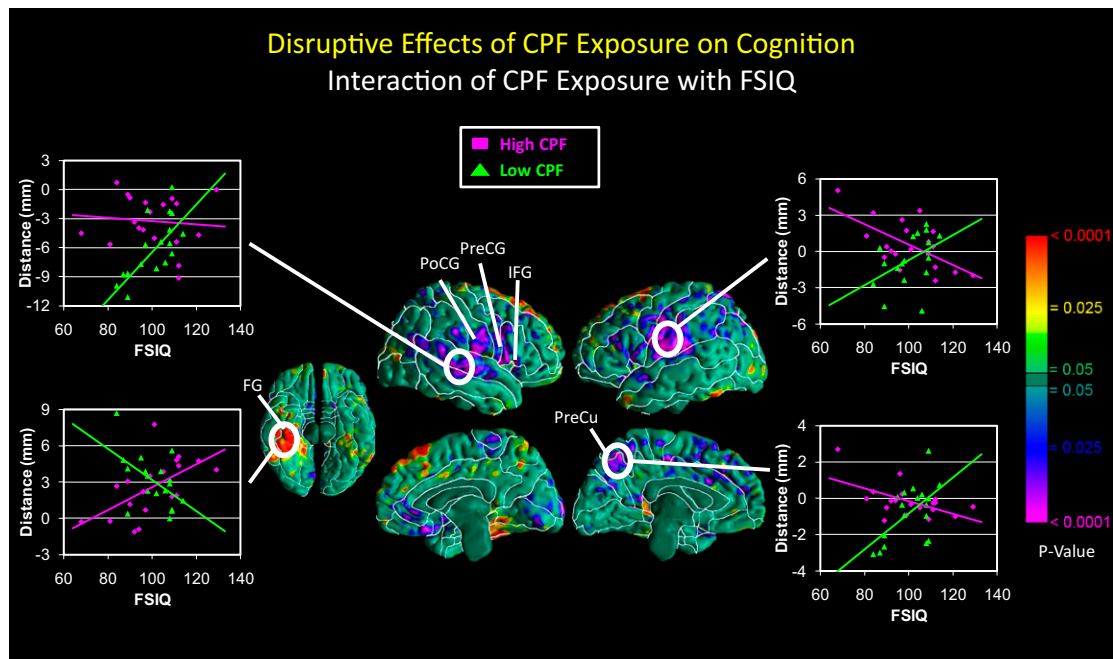


Fig. 2. Correlations of surface measures with full-scale IQ in high- vs. low-CPF exposure groups. Surface distances (in mm from the corresponding point on the surface of the template brain), adjusted for age and sex, are plotted on the y axis. Surface measures in the superior temporal, inferior frontal, inferior precentral, and inferior postcentral gyri bilaterally, and the precuneus of the left hemisphere, correlated positively with full-scale IQ in the low- but not the high-CPF group, producing a significant IQ \times exposure interaction. Scatterplots (pink denotes high and green denotes low exposure) suggest that high CPF exposure was associated with enlargement of these regions, consistent with findings for the main effects of CPF on surface measures (Fig. 1), also indicating that those regional enlargements were associated with lower IQ scores in the high-CPF group. Distances in the right fusiform gyrus correlated inversely with IQ in the low-CPF group, but positively in the high group, also producing a significant IQ \times exposure interaction. FG, fusiform gyrus; FSIQ, full-scale IQ; IFG, inferior frontal gyrus; PoCG, postcentral gyrus; PreCG, precentral gyrus; PreCu, precuneus.

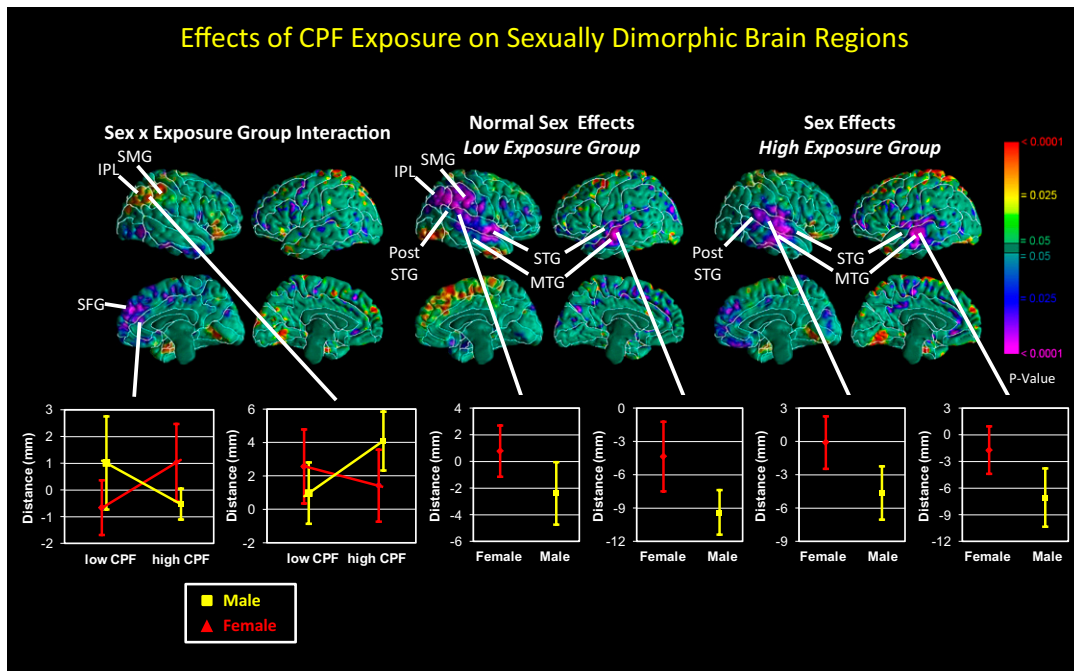


Fig. 3. Maps of differences in local cortical surface measures by sex and prenatal CPF exposure level in sexually dimorphic brain regions. (*Upper Left*) Sex \times exposure interaction, indicating a loss in the high-CPF group of normal female-larger-than-male sex effects in the right inferior parietal lobule and supramarginal gyrus, and reversal of normal male-larger-than-female effects in the right mesial superior frontal gyrus. (*Upper Center*) shows normal female-larger-than-male effects (purple) in the inferior parietal lobule, supramarginal gyrus, and middle and superior temporal gyri in the low-CPF group, and normal male-larger-than-female effects in the right mesial superior frontal gyrus in the low CPF group. (*Upper Right*) shows less extensive but similar effects in the high-CPF group. In the corresponding graphs (*Lower*), surface distances (in mm from the corresponding point on the surface of the template brain) are plotted on the y axis. Male data are coded yellow and female red. Error bars represent SEs. IPL, inferior parietal lobule; MTG, middle temporal gyrus; SFG, superior frontal gyrus; SMG, supramarginal gyrus; STG, superior temporal gyrus. High-CPF group: $n = 19$; low-CPF group: $n = 18$.

differences in the right parietal lobe and a reversal of normal, male-larger-than-female differences in the right mesial superior frontal gyrus (Fig. 3). Within the right dorsal parietal lobe of the high-CPF group, we also found a significant sex \times CPF interaction, in which CPF levels correlated positively with surface measures in girls but inversely in boys (Fig. 3).

Cortical thickness. We detected scattered reductions in cortical thickness in dorsal parietal and frontal cortices in the high- vs. low-exposure group (Fig. S4). Within the high group, we saw an inverse dose–response relationship of cortical thickness with CPF, in which thinner cortices were associated bilaterally with higher exposures in the frontal pole, dorsal parietal, and orbitofrontal cortices (Fig. S5).

Discussion

Our findings indicate that prenatal CPF exposure, at levels observed with routine (nonoccupational) use and below the threshold for any signs of acute exposure, has a measureable effect on brain structure in a sample of 40 children 5.9–11.2 y of age. We found significant abnormalities in morphological measures of the cerebral surface associated with higher prenatal CPF exposure, after adjusting for possible confounders. Regional enlargements of the cerebral surface predominated and were located in the superior temporal, posterior middle temporal, and inferior postcentral gyri bilaterally, and in the superior frontal gyrus, gyrus rectus, cuneus, and precuneus along the mesial wall of the right hemisphere (Fig. 1). The enlargements derived primarily from enlargements of underlying white matter. The cognitive and behavioral processes that these cortical regions subserve include attention and receptive language in the posterior temporal regions (24); social cognition in the mesial superior frontal gyrus, cuneus, and precuneus (25), and superior temporal gyrus (26); and reward, emotion, and inhibitory control in the

gyrus rectus and related orbitofrontal regions (27). Inward deformations were detected in the dorsal and mesial surfaces of the left superior frontal gyrus, a region supporting executive functioning. A positive dose–response relationship between CPF concentrations and surface measures was detected in the mesial portion of the superior frontal gyrus bilaterally.

These findings are consistent with the effects of early developmental exposure to CPF in animal models. CPF exposure is cytotoxic to both glia and neurons (18–20, 28), and the signs of neural damage include excessive astrocytic processes and perikaryal swelling, progressing to more extensive astrogliosis and glial scarring in response to the earlier cellular injury (19, 29). The white matter origins of the abnormalities in local cortical volumes seen here may thus represent similar glial scarring as an effect of prenatal exposure in humans. Likewise, the direct neurotoxic effects of early CPF exposure in animals include altered neuronal cell replication, apoptosis, and cortical lamination (18, 19, 30), providing a highly plausible cellular basis for the dose-related cortical thinning that we detected bilaterally in dorsal parietal, frontal, and orbitofrontal cortices of the high-exposure group. The exposures at which these mechanisms become manifest in animal models are comparable to exposure levels in our own population.

In addition, we found evidence for a detrimental effect of exposure on general cognition that was likely mediated by the effects of CPF on surface measures of the superior temporal and inferior frontal cortices. We found a significant IQ \times exposure interaction effect on surface measures in the superior temporal gyrus and inferior portions of the precentral, postcentral, and inferior frontal gyri (Fig. 2). This interaction derived from significant positive correlations of surface measures with IQ in the low-CPF group that were disrupted in the high group. Scatterplots of this interaction suggest that these regions were significantly enlarged in the high-CPF group (Fig. 2), particularly for those with lower IQ

scores, consistent with findings for the main effects of CPF on surface measures (Fig. 1) and with prior reports that prenatal CPF exposure is associated with child cognitive impairment (15–17).

The high-CPF group also displayed disruption of normal sexual dimorphisms in brain structure—features that were preserved in the low-CPF group, including enlargement of the right inferior parietal lobule, supramarginal gyrus, and bilateral superior and middle temporal gyri in females (31, 32), and enlargement of the left mesial surface of the superior frontal gyrus in males (33). These expected sex differences were reversed in the high-CPF group. Our morphological findings are consistent with those from animal models showing that early CPF exposure obtunds or reverses normal sex differences in learning, memory, and emotional behaviors (21, 22, 34). In the cohort from which this sample was drawn, prenatal CPF exposure was shown to have an inverse dose–response effect on cognition (working memory scores and, to a lesser extent, full-scale IQ) among 264 7-y-old children (17). Because the dorsolateral prefrontal cortex subserves cognitive processes, including working memory, we suspect that the impaired cognitive scores associated with prenatal CPF exposure in the larger cohort likely derived from either reduced surface morphological measures (Fig. 1) or dose-related thinning (Fig. S5) in the prefrontal cortex that were detected in our high-exposure group.

Our study has several limitations. First, the modest sample size ($n = 40$) made it difficult to detect within-group correlations and to test multiple interactions of exposure with other variables. The sample size was limited by our requirement that participants have minimal or no prenatal exposure to ETS and PAH—known neurotoxicants and potential confounders in our assessment of the neurodevelopmental effects of CPF. We believe that the sample size nevertheless permits generalization of our findings to a larger urban population, because it was a representative community-based sample. Second, the cognitive assessment was limited to a standard, broadband performance measure. More sensitive and functionally specific measures of cognitive and behavioral functioning may yield more anatomically relevant correlations of those measures with regional effects of CPF on brain structure. Finally, genetic polymorphisms have recently been shown to influence the rates of organophosphate metabolism in humans (15, 16), and those genotype data were unavailable for this study.

Despite these limitations, our findings of altered brain development in children exposed to CPF in utero have important public health implications. First, associations between prenatal exposure, brain structure, and neurocognitive alterations at 5.9–11.2 y of age suggest that the neurotoxic effects of CPF are long term, at least extending into the early school years. The persistence of effects is consistent with animal studies suggesting that CPF effects are irreversible (35). Second, the high-exposure group (using a cut point of 4.39 pg/g) had relatively modest doses of CPF—doses that were measurable only because of the remarkable sensitivity of the CPF assay (36). Specimens from a Cincinnati blood bank during the same time period (36) showed a background CPF concentration of 9 pg/g in serum (twice the mean level reported here), suggesting that exposure concentrations in the present sample were not unusually high. Current safety limits are set according to levels needed to achieve inhibition of plasma cholinesterase, a surrogate for inhibition of acetylcholinesterase in the brain, long assumed to be the common mechanism by which organophosphates induce neurodevelopmental deficits. However, pathogenic mechanisms other than cholinesterase inhibition are almost certainly contributing to the deleterious effects of early exposure to organophosphates (21, 37), including the observed brain abnormalities and their accompanying cognitive deficits. Human exposure limits based on the detection of cholinesterase inhibition may therefore be insufficient to protect brain development in exposed children.

Although residential application of CPF was banned in 2001, our findings of altered brain development and cognitive effects

associated with prenatal exposure to CPF are cause for concern because widespread agricultural use of CPF continues unabated. Many pregnant women and young children thus continue to be exposed to high levels of CPF, possibly higher than those observed in the present study, whereas the general population continues to receive lower exposures through ingestion of CPF residues on agricultural products.

Methods

Participants and Procedures. Participants were recruited from a prospective cohort study conducted by the Columbia Center for Children's Environmental Health (38) to evaluate the effects of prenatal exposures to air pollutants on neurodevelopment in children from low-income urban communities. Non-smoking African American or Dominican women, aged 18–35, and registered at New York Presbyterian Medical Center or Harlem Hospital prenatal clinics by the 20th week of pregnancy, were approached for consent. Eligible women were low risk (free of diabetes, hypertension, known HIV, and documented drug abuse), and resident in the area for at least 1 y.

Exposure Assessment. Umbilical cord blood (30–60 mL) was collected at delivery and portions sent to the Centers for Disease Control for analysis of plasma levels of CPF, cotinine, and metals, as described elsewhere (39). Methods for the laboratory assay for CPF (quality control, limits of detection) are previously published (36). The high-CPF group included upper tertile exposures (≥ 4.39 pg/g); the low group included exposures below this level. Prenatal ETS exposure was classified by maternal report validated by cord-blood cotinine levels (< 15 ng/mL) (23). We measured PAH exposure by third-trimester personal-air monitoring, excluding poor-quality samples; low exposure was defined as below the median (2.26 ng/m³) (40). Cord-blood lead concentrations ($\mu\text{g/dL}$) were available in subsets of the sample ($n = 28$) and the larger cohort ($n = 202$).

MRI Acquisition. High-resolution, T1-weighted anatomical images were acquired using a GE Signa 3 Tesla whole-body scanner with an eight-channel head receiver coil and a fast spoiled-gradient recall sequence (*SI Methods*).

Image Processing. All processing was conducted on Sun Ultra 10 workstations using ANALYZE 8.0 Biomedical Imaging Resource (Mayo Foundation, Rochester, MN) and in-house software, blind to participant characteristics and hemisphere (images were randomly flipped in the transverse plane before preprocessing). Morphometric analyses were performed with the MRI dataset resliced to correct for residual head rotation, tilt, or flexion/extension.

Preprocessing. Large-scale variations in image intensity were corrected by an algorithm developed at the Montreal Neurological Institute (41). Extracerebral tissues were removed by an automated tool (42) that uses an anisotropic filter to smooth image intensity, and a Marr–Hildreth edge detector (43) to identify 3D edges, before selecting as the brain the largest connected component with a closed boundary. Connecting dura was removed manually on each sagittal slice and checked in orthogonal views. The brainstem was transected at the pontomedullary junction.

Cortical gray matter segmentation. Gray-scale values of “pure” representations of cortical gray and white matter were sampled bilaterally at four standard brain locations (frontal, temporal, occipital, and parietal) using $8 \times 8 = 64$ pixel array, large enough for statistical stability but small enough to avoid partial volume effects, including other tissue types. *SI Methods* detail the computation of threshold values for classification of cortical gray and white matter (44).

Morphological maps of the cerebral surface. Detailed procedures used to analyze surface morphologies, and their related validation studies, appear elsewhere (45, 46) and in *SI Methods*.

Cortical thickness. From the coregistered brain of each child we subtracted its cortical mantle, and used a 3D morphological operator to distance transform this brain without the cortex from the coregistered brain of the same child that contained the cortex (47, 48). Operation details appear in *SI Methods*.

Choice of template brain. We first identified a brain, representative of the sample by child age, weight, and height. Brains for the remaining participants were coregistered to this preliminary template. We determined point correspondences on cortical surfaces, and computed distances of corresponding points on the cerebral surface of other participants from the template surface. The brain for which all points across the surface are closest to the average of computed distances (by least squares) was selected as the final template. Brains underwent a second coregistration to this representative template. We used a single representative template rather than an averaged brain because it has well-defined tissue interfaces (e.g., CSF/gray matter or gray/white matter interfaces). Averaging images for a template blurs these

boundaries and increases registration errors important for distinguishing subtle effects across populations.

Sulcal overlay. To aid visual identification of findings on the brain surface, we overlaid onto our template maps the sulcal boundaries and 3D labels of cortical gyri identified on the International Consortium for Brain Mapping high-resolution, single-participant template (49), using a high-dimensional, nonrigid warping algorithm.

Cognitive Assessment. To assess IQ at 7 y (± 1 mo), we used the Wechsler Scales of Intelligence for Children (WISC-IV) (50), which is sensitive to low-dose neurotoxic exposures in studies of lead toxicity in 6- to 7.5-y-old children (51). The instrument measures overall IQ and four areas of cognitive functioning (verbal comprehension, perceptual reasoning, processing speed, and working memory) that are associated with, but distinct from, overall IQ, and is sensitive to cognitive deficits related to learning and working memory that have been linked to CPF exposure in rodent studies (22).

Statistical Analysis. Each imaging measure (Euclidean distance or cortical thickness) was subjected to statistical modeling at each voxel of the cortical surface of the template brain. We used general linear modeling to compare measures across CPF groups, covarying for age and sex. *P* values were corrected for multiple comparisons using a false discovery rate $P < 0.05$ (52), then color-coded and plotted for each voxel at the cerebral surface. We assessed correlations of surface distances and cortical thickness with measures of CPF exposure and full-scale IQ at each voxel across the brain surface.

ACKNOWLEDGMENTS. We are grateful to the families of northern Manhattan who have so generously contributed their time and effort to the study. This study was supported by National Institute of Environmental Health Sciences Grants 5P01ES09600, P50ES015905, and 5R01ES08977, as well as pilot funding through ES009089; US Environmental Protection Agency STAR Grants RD834509, RD832141, and R827027; National Institute of Mental Health Grants MH068318 and K02-74677; and the John and Wendy Neu Family Foundation.

1. US Environmental Protection Agency (2000) *Chlorpyrifos Revised Risk Assessment and Agreement with Registrants* (US Environmental Protection Agency, Washington, DC).
2. Berkowitz GS, et al. (2003) Exposure to indoor pesticides during pregnancy in a multiethnic, urban cohort. *Environ Health Perspect* 111:79–84.
3. Whyatt RM, et al. (2002) Residential pesticide use during pregnancy among a cohort of urban minority women. *Environ Health Perspect* 110:507–514.
4. Slotkin TA (2004) Guidelines for developmental neurotoxicity and their impact on organophosphate pesticides: A personal view from an academic perspective. *Neurotoxicology* 25:631–640.
5. Mauro RE, Zhang L (2007) Unique insights into the actions of CNS agents: Lessons from studies of chlorpyrifos and other common pesticides. *Central Nerv Syst Agents Med Chem* 7(3):183–199.
6. Bradman A, et al. (2003) Measurement of pesticides and other toxicants in amniotic fluid as a potential biomarker of prenatal exposure: A validation study. *Environ Health Perspect* 111:1779–1782.
7. Whyatt RM, et al. (2005) Biomarkers in assessing residential insecticide exposures during pregnancy and effects on fetal growth. *Toxicol Appl Pharmacol* 206:246–254.
8. Berkowitz GS, et al. (2004) In utero pesticide exposure, maternal paraoxonase activity, and head circumference. *Environ Health Perspect* 112:388–391.
9. Whyatt RM, et al. (2004) Prenatal insecticide exposures and birth weight and length among an urban minority cohort. *Environ Health Perspect* 112:1125–1132.
10. Engel SM, et al. (2007) Prenatal organophosphate metabolite and organochlorine levels and performance on the Brazelton Neonatal Behavioral Assessment Scale in a multiethnic pregnancy cohort. *Am J Epidemiol* 165:1397–1404.
11. Young JG, et al. (2005) Association between in utero organophosphate pesticide exposure and abnormal reflexes in neonates. *Neurotoxicology* 26:199–209.
12. Marks AR, et al. (2010) Organophosphate pesticide exposure and attention in young Mexican-American children: The CHAMACOS study. *Environ Health Perspect* 118:1768–1774.
13. Rauh VA, et al. (2006) Impact of prenatal chlorpyrifos exposure on neurodevelopment in the first 3 years of life among inner-city children. *Pediatrics* 118(6):e1845–e1859.
14. Eskenazi B, et al. (2007) Organophosphate pesticide exposure and neurodevelopment in young Mexican-American children. *Environ Health Perspect* 115:792–798.
15. Bouchard MF, et al. (2011) Prenatal exposure to organophosphate pesticides and IQ in 7-year-old children. *Environ Health Perspect* 119:1189–1195.
16. Engel SM, et al. (2011) Prenatal exposure to organophosphates, paraoxonase 1, and cognitive development in childhood. *Environ Health Perspect* 119:1182–1188.
17. Rauh VA, et al. (2011) Seven-year neurodevelopmental scores and prenatal exposure to chlorpyrifos, a common agricultural pesticide. *Environ Health Perspect* 119:1196–1201.
18. Roy TS, Seidler FJ, Slotkin TA (2004) Morphologic effects of subtoxic neonatal chlorpyrifos exposure in developing rat brain: regionally selective alterations in neurons and glia. *Brain Res Dev Brain Res* 148:197–206.
19. Roy TS, Sharma V, Seidler FJ, Slotkin TA (2005) Quantitative morphological assessment reveals neuronal and glial deficits in hippocampus after a brief subtoxic exposure to chlorpyrifos in neonatal rats. *Brain Res Dev Brain Res* 155:71–80.
20. Garcia SJ, Seidler FJ, Qiao D, Slotkin TA (2002) Chlorpyrifos targets developing glia: Effects on glial fibrillary acidic protein. *Brain Res Dev Brain Res* 133:151–161.
21. Aldridge JE, Seidler FJ, Slotkin TA (2004) Developmental exposure to chlorpyrifos elicits sex-selective alterations of serotonergic synaptic function in adulthood: Critical periods and regional selectivity for effects on the serotonin transporter, receptor subtypes, and cell signaling. *Environ Health Perspect* 112:148–155.
22. Levin ED, et al. (2001) Persistent behavioral consequences of neonatal chlorpyrifos exposure in rats. *Dev Brain Res* 130:83–89.
23. Rauh VA, et al. (2004) Developmental effects of exposure to environmental tobacco smoke and material hardship among inner-city children. *Neurotoxicol Teratol* 26:373–385.
24. Adler CM, et al. (2001) Changes in neuronal activation with increasing attention demand in healthy volunteers: An fMRI study. *Synapse* 42:266–272.
25. Forbes CE, Grafman J (2010) The role of the human prefrontal cortex in social cognition and moral judgment. *Annu Rev Neurosci* 33:299–324.
26. Bigler ED, et al. (2007) Superior temporal gyrus, language function, and autism. *Dev Neuropsychol* 31:217–238.
27. Elliott R, Deakin B (2005) Role of the orbitofrontal cortex in reinforcement processing and inhibitory control: Evidence from functional magnetic resonance imaging studies in healthy human subjects. *Int Rev Neurobiol* 65:89–116.
28. Garcia SJ, Seidler FJ, Crumpton TL, Slotkin TA (2001) Does the developmental neurotoxicity of chlorpyrifos involve glial targets? Macromolecule synthesis, adenylyl cyclase signaling, nuclear transcription factors, and formation of reactive oxygen in C6 glioma cells. *Brain Res* 891:54–68.
29. O'Callaghan JP, Miller DB (1993) Quantification of reactive gliosis as an approach to neurotoxicity assessment. *NIDA Res Monogr* 136:188–212.
30. Slotkin TA (2005) Developmental neurotoxicity of organophosphates: A case study of chlorpyrifos. *Toxicity of Organophosphate and Carbamate Pesticides*, ed Gupta RC (Elsevier Academic, San Diego), pp 293–314.
31. Harasty J, Double KL, Halliday GM, Kril JJ, McRitchie DA (1997) Language-associated cortical regions are proportionally larger in the female brain. *Arch Neurol* 54:171–176.
32. Nopoulos P, Flaum M, O'Leary D, Andreasen NC (2000) Sexual dimorphism in the human brain: Evaluation of tissue volume, tissue composition and surface anatomy using magnetic resonance imaging. *Psychiatry Res* 98:1–13.
33. Cahill L (2006) Why sex matters for neuroscience. *Nat Rev Neurosci* 7:477–484.
34. Aldridge JE, Levin ED, Seidler FJ, Slotkin TA (2005) Developmental exposure of rats to chlorpyrifos leads to behavioral alterations in adulthood, involving serotonergic mechanisms and resembling animal models of depression. *Environ Health Perspect* 113:527–531.
35. Slotkin TA, Seidler FJ (2005) The alterations in CNS serotonergic mechanisms caused by neonatal chlorpyrifos exposure are permanent. *Brain Res Dev Brain Res* 158:115–119.
36. Barr DB, et al. (2002) A multi-analyte method for the quantification of contemporary pesticides in human serum and plasma using high-resolution mass spectrometry. *J Chromatogr B Analyt Technol Biomed Life Sci* 778:99–111.
37. Casida JE, Quistad GB (2004) Organophosphate toxicology: Safety aspects of non-acetylcholinesterase secondary targets. *Chem Res Toxicol* 17:983–998.
38. Perera FP, et al. (2002) The challenge of preventing environmentally related disease in young children: Community-based research in New York City. *Environ Health Perspect* 110:197–204.
39. Whyatt RM, et al. (2003) Contemporary-use pesticides in personal air samples during pregnancy and blood samples at delivery among urban minority mothers and newborns. *Environ Health Perspect* 111:749–756.
40. Perera FP, et al. (2003) Effects of transplacental exposure to environmental pollutants on birth outcomes in a multiethnic population. *Environ Health Perspect* 111:201–205.
41. Sled JG, Zijdenbos AP, Evans AC (1998) A nonparametric method for automatic correction of intensity nonuniformity in MRI data. *IEEE Trans Med Imaging* 17:87–97.
42. Shattuck DW, Leahy RM (2002) BrainSuite: An automated cortical surface identification tool. *Med Image Anal* 6:129–142.
43. Marr D, Hildreth E (1980) Theory of edge detection. *Proc R Soc Lond B Biol Sci* 207:187–217.
44. Shrout PE, Fleiss JL (1979) Intraclass correlations: Uses in assessing rater reliability. *Psychol Bull* 86:420–428.
45. Bansal R, Staib LH, Whiteman R, Wang YM, Peterson BS (2005) ROC-based assessments of 3D cortical surface-matching algorithms. *Neuroimage* 24:150–162.
46. Plessen KJ, et al. (2006) Hippocampus and amygdala morphology in attention-deficit/hyperactivity disorder. *Arch Gen Psychiatry* 63:795–807.
47. Haralick R, Shapiro L (1992) *Computer and Robot Vision* (Addison-Wesley, Reading, MA), Vol 1, Chap 5.
48. Rosenfeld A, Pfaltz J (1968) Distance functions in digital pictures. *Pattern Recognit* 1:33–61.
49. Mazziotta J, et al. (2001) A probabilistic atlas and reference system for the human brain: International Consortium for Brain Mapping (ICBM). *Philos Trans R Soc Lond B Biol Sci* 356:1293–1322.
50. Wechsler D (2003) *Wechsler Intelligence Scale for Children. Administration and Scoring Manual* (Harcourt Assessment, Inc., San Antonio, TX), 4th Ed.
51. Chiodo LM, Jacobson SW, Jacobson JL (2004) Neurodevelopmental effects of post-natal lead exposure at very low levels. *Neurotoxicol Teratol* 26:359–371.
52. Benjamini Y, Hochberg Y (1995) Controlling the false discovery rate: A practical and powerful approach to multiple testing. *J Royal Stat Soc B* 57:289–300.
53. Brown L, Sherbenou RJ, Johnson SK (1997) *Test of Nonverbal Intelligence* (Pro-Ed, Austin, TX), 3rd Ed.